



Effect of V₂O₅ incorporation on the Structural, Electrical, and Conduction Properties of sulfonated PVC/PMMA Blend: Positron Annihilation Study



Mohamed R. M. Elsharkawy*, Sona Ibrahim and Wael M. Mohammed

Physics Department, Faculty of Science, Minia University, P.O. Box 61519 Minai, Egypt;
waelmohamed@mu.edu.eg, mrmelsharkawy@mu.edu.eg wm15516@gmail.com

Abstract

The present study investigates the structural, electrical, and free volume properties of PVC/PMMA blends modified with V₂O₅ filler using various characterization techniques. X-ray diffraction (XRD) analysis reveals that the addition of V₂O₅ does not significantly alter the peak positions but decreases the intensity and broadens the peaks, indicating a slight decrease in the degree of crystallinity. The AC conductivity of the PVC/PMMA/V₂O₅ blend is lower compared to the PVC/PMMA blend, attributed to the dielectric properties of V₂O₅, which increase the overall dielectric constant and reduce the AC conductivity. The conduction mechanism is identified as the correlated barrier hopping (CBH) mechanism, where charge carriers require energy to travel through the material. Impedance spectroscopy shows a semicircle representing Debye relaxation, a constant phase element, and an inductive element. The DC ionic conductivity of the PVC/PMMA/V₂O₅ blend is lower than the PVC/PMMA blend, explained by strong interactions between V₂O₅ and polymer chains, restricting mobility and segmental motion essential for ionic transport. Positron annihilation lifetime spectroscopy (PALS) indicates that adding V₂O₅ decreases the average free volume size and increases the free volume fraction, attributed to the reinforcement effect of V₂O₅, which restricts segmental motion and alters free volume characteristics. The findings provide valuable insights into structure-property relationships in PVC/PMMA/V₂O₅ blends, with implications for designing advanced polymer-based materials with tailored electrical and free volume properties for applications in energy storage, sensors, and optoelectronics.

Introduction

Proton exchange membranes (PEMs) are crucial components in fuel cells, playing a pivotal role in the efficiency and functionality of these energy conversion devices. The development and optimization of PEMs often involves the integration of advanced materials to enhance their properties. Among these materials, vanadium pentoxide (V₂O₅), polyvinyl chloride (PVC), and polymethyl methacrylate (PMMA) have shown significant potential. For a membrane to exhibit proton conductivity, it must contain an active group, such as the sulfonic acid group (SO₃H). The incorporation of the SO₃H group has a substantial influence on the membrane's physicochemical properties. Moreover, the structure of the free volume is crucial, as it modifies the free volume and creates additional pathways for ion transport. This modification directly impacts and enhances ionic conductivity [1-3].

*Correspondence: Mohamed R. M. Elsharkawy1, E-mail: mrmelsharkawy@mu.edu.eg, Tel. +201001559562

Received: 30/06/2024; Accepted: 14/07/2024

DOI: 10.21608/EJPHYSICS.2024.300434.1102

©2024 National Information and Documentation Center (NIDOC)

Vanadium pentoxide (V_2O_5) is a multifaceted material recognized for its exceptional electrochemical, catalytic, and optical properties. Its ability to transition between different oxidation states makes it indispensable in various industrial and technological applications. For instance, V_2O_5 is extensively used in catalysis, notably in the production of sulfuric acid and in the selective catalytic reduction (SCR) of nitrogen oxides in automotive exhaust systems, which helps in reducing environmental pollution. Furthermore, V_2O_5 is vital in the energy sector, particularly in the development of lithium-ion and sodium-ion batteries. Its high capacity for lithium and sodium insertion enhances the performance and longevity of these batteries, making them more efficient and durable [4,5]. V_2O_5 also plays a crucial role in the field of renewable energy, especially in the development of proton exchange membranes (PEMs) for fuel cells. V_2O_5 can improve the proton conductivity and thermal stability of PEMs, leading to higher efficiency and durability in fuel cells. This enhancement is essential for the broader adoption of fuel cells in clean energy applications, contributing to the reduction of greenhouse gas emissions and the transition to sustainable energy sources. The material's high refractive index and thermal stability also make it suitable for optical applications, including smart windows and electrochromic devices, which regulate light and heat transmission [6].

Sulfonation of polymers such as PMMA and PVC using sulfonating agents like sulfonated succinic acid (SSA) significantly enhances their ionic conductivity and mechanical properties. Introducing sulfonic acid groups into the polymer matrix increases hydrophilicity, proton conductivity, and thermal stability, making these sulfonated polymers ideal for advanced applications. Sulfonated PMMA/PVC membranes are particularly valuable in energy-related applications, serving as proton exchange membranes in fuel cells. These membranes facilitate efficient proton transport while preventing fuel crossover, thereby improving fuel cell efficiency and durability. Additionally, sulfonated polymers are used in water treatment as ion-exchange membranes due to their high chemical resistance and selective permeability [7]. Polyvinyl chloride (PVC) offers strong mechanical strength and chemical resistance, while polymethyl methacrylate (PMMA) provides optical clarity and weather resilience. Blending these polymers creates materials with balanced properties. Positron annihilation techniques reveal the free volume within PVC/PMMA blends, crucial for optimizing their mechanical, thermal, and barrier properties. Non-fluorinated PVA/SSA proton exchange membranes have shown significant fuel cell improvements, underscoring the importance of PEMs in renewable energy technologies [8].

Positron Annihilation Lifetime Spectroscopy (PALS) is a highly effective technique for analyzing the microstructural characteristics of materials, particularly polymers. The method involves injecting positrons into a material, where they may form positronium (Ps), a bound state of a positron and an electron. The annihilation of positronium results in the emission of gamma rays, and the time taken for this annihilation, known as the positronium lifetime, is influenced by the size and distribution of free volumes or voids within the material. This sensitivity makes PALS an invaluable tool for probing nanoscale voids in polymers, providing detailed information about the size, content, and distribution of these free-volume holes [9, 10]. The PALS technique capitalizes on the trapping of positronium atoms in atomic-scale voids, typically ranging from 1 to 10 Å in size. The different lifetimes and intensities of positronium states provide critical insights into the size and distribution of these free volumes. The ortho-positronium (o-Ps) lifetime (τ_3) and its intensity (I_3) are particularly indicative of the characteristics of free-volume holes. By analyzing these parameters, researchers can determine the size and distribution of free volumes, which are directly linked to the material's macroscopic properties such as

mechanical strength, thermal stability, and permeability. The theoretical framework of PALS involves the Tao-Eldrup model, which correlates the o-Ps lifetime with the radius of spherical free volumes in the material. This model suggests that the annihilation lifetime is a function of the void size, enabling quantitative assessment of free volumes. Despite the model's assumption of spherical voids, it provides a good approximation for average hole sizes and their distribution. Advanced analysis techniques, such as continuous lifetime spectrum analysis, further enhance the understanding of the microstructure of free volumes and their impact on material properties [11-13].

The incorporation of vanadium pentoxide (V₂O₅) into a polymethyl methacrylate (PMMA) and polyvinyl chloride (PVC) polymer blend offers several significant advantages that enhance the material's performance, particularly for applications in energy storage and electronic devices. V₂O₅ contributes to the mechanical robustness of the PMMA/PVC blend by reinforcing the polymer matrix, thus improving its strength and stability under various operational conditions. This enhancement is crucial for the durability of materials used in demanding environments. The incorporation of V₂O₅ can also lead to a more favorable morphology of the polymer blend, including better dispersion of the polymer phases and improved interaction between PMMA and PVC. This results in enhanced material properties, which are essential for high-performance applications [14]. Additionally, V₂O₅ exhibits excellent catalytic properties, which can be leveraged in applications requiring catalytic activity, such as sensors or the catalytic layers of fuel cells. This addition promotes reactions that improve the overall efficiency of these devices [15, 16].

This work aims to investigate the effects of vanadium pentoxide (V₂O₅) on the dielectric characteristics of sulfonated PVC/PMMA blends, as well as the ortho-positronium lifetime and the free volume holes size. The study investigates how these additives modify the dielectric and microstructural properties of the polymer composites by introducing V₂O₅. Positron annihilation lifetime spectroscopy (PALS) and X-ray diffraction (XRD) are used to assess these changes. Dielectric measurements will evaluate the impact of these additives on dielectric constant and loss across various frequencies. Additionally, Fourier-transform infrared spectroscopy (FTIR), ion exchange capacity (IEC), and water uptake measurements are conducted to provide a comprehensive understanding. This work seeks to uncover the fundamental mechanisms driving these changes and establish correlations between microstructural modifications and macroscopic properties, contributing to the development of high-performance polymer composites for advanced technological applications.

Materials and Methods

Materials

The primary chemicals used are polymethyl methacrylate (PMMA) [(C₅H₈O₂)_n; density: 1.18 g/cm³] of molecular weight 40,000 and polyvinyl chloride (PVC) [(C₂H₃Cl)_n; density: 1.39 g/cm³] provided by Merck, Germany. The 70 wt. % SSA solution was purchased from Aldrich and utilized without being purified. The V₂O₅ supplied by Alpha, with a density of 3.36 g/cm³ and a molecular mass of 181.88 g/mol, was added to the PVC/PMMA blend as filler.

Preparation of PMMA/PVC membrane

PVC/PMMA composites were produced in the following ways using the casting method: To remove any moisture from the polymers, sections of PVC and PMMA were dried in a vacuum oven for about an hour at 55 °C before being employed. Polyvinyl chloride (PVC) and polymethyl methacrylate (PMMA) were dissolved in tetrahydrofuran with a weight ratio of 70:30, respectively. At 60 °C, the mixture was agitated for about 6 hours to produce a consistent, thick liquid solution. 30 wt% of SSA was introduced into the mix solution. After that, the suspension was agitated for 24 hours with the addition of 0.5 wt. % of V₂O₅ nanoparticles, until a clear solution was achieved. The homogenous solutions were poured into glass Petri dishes and subsequently left to air dry. After being dried, the films were taken out of the Petri dishes and kept in vacuum-sealed containers until they were needed. The films were suitably separated into portions for measuring. The films that are produced are around 40 mm thick.

X-ray spectroscopy

By using X-ray diffraction (XRD), a deeper understanding of the crystalline properties of the materials under study was attained. The measurements were taken using a Joel JSX-600 PA diffractometer with CuK α incident radiation ($\lambda = 1.54184 \text{ \AA}$). Within a 2θ range, the recorded WAXD peaks varied from 5 to 100°.

Fourier transform infrared spectroscopy

The chemical structure of PVC/PMMA sulfonated membranes and sulfonated PVC/PMMA filled with V₂O₅ was analyzed via FTIR. The membrane's functional groups were assessed using a Bruker Alpha FTIR spectrometer (USA), spanning wavenumbers from 4000 to 400 cm⁻¹ with a resolution of 0.9 cm⁻¹ at a temperature of 25°C

Ion exchange capacity (IEC)

The IEC for sulfonated PVC/PMMA membranes and the filled PVC/PMMA with V₂O₅ was calculated by applying the recognized acid-base volumetric titration method utilizing phenolphthalein as the indicator. The investigated membranes were dried for one day under vacuum, then they immersed in 25 ml of 3 M NaCl solution for 24 h. Thereafter, 10 ml of this solution was titrated with 0.05 M NaOH. A 0.05 M NaOH was dropped to the solution until the solution color was changed to pink. In units of mmol (NaOH)/gram of polymer, IEC was calculated from the titration results using the following equation [17, 18]

$$IEC = \frac{0.05 \times V_{NaOH} \times n}{W_{dry}} (\text{mmole/gm})$$

Where V_{NaOH} is the volume of 0.05 M NaOH solution, n is a factor corresponding to the ratio of the amount of NaCl used for the immersion of the polymer to the amount used for the titration (2.5), and W_{dry} is the dry membrane weight. Fig. 1 illustrates the relationship between IEC calculated values and SSA ratios for PVC/PMMA blend samples at varying sulfonation levels. As shown in the table, the highest value of IEC was obtained at 30 wt.% of SSA. These results led us to choose the PVC/PMMA/SSA (30 wt.%) for conducting our study.

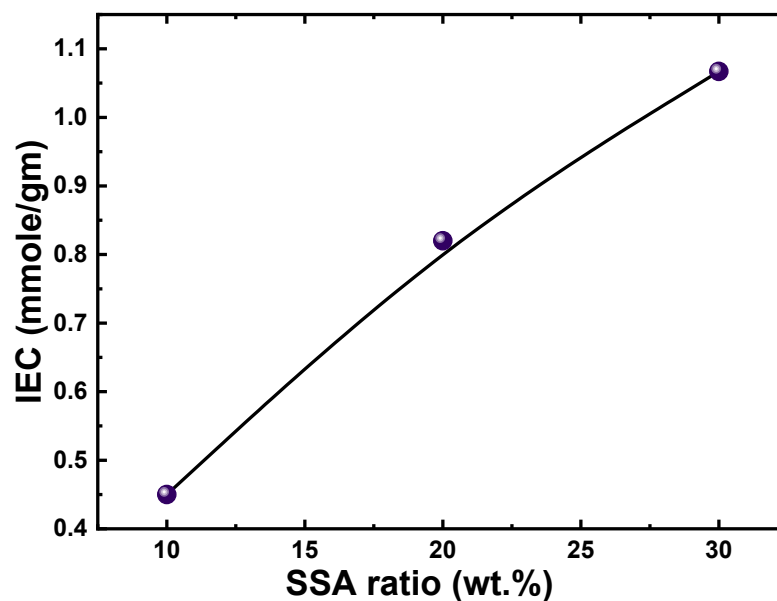


Fig. 1: Variation of IEC with SSA ration

Positron annihilation lifetime spectroscopy (PALS)

(PAL) measurements were carried out on all samples at room temperature (25°C) using a fast-fast coincidence system with a time resolution of 250 ps. A 20 μ Ci ²²Na positron source was applied to Kapton foil and subsequently sandwiched between two identical sample pieces. Over a million counts were accumulated in five hours for each PAL spectrum measurement. The Tao-Eldrup model [19] describes the link between the average radius of the hole volume size (R) and the o-Ps lifetime (τ_3) within a spherical approximation as:

$$\tau_3 = 0.5 \left\{ 1 - \frac{R}{R_0} + \frac{1}{2\pi} \sin\left(\frac{2\pi R}{R_0}\right) \right\}^{-1} \quad (1)$$

This formula emphasizes the clear relationship between the free volume in the polymer matrix and the o-Ps lifetime, offering a crucial parameter for the description of polymeric materials. Where $\Delta R = 0.166$ nm, the thickness of the homogenous electron layer where the positron in o-Ps annihilates, and $R_0 = R + \Delta R$. The following formula can be used to get the hole volume size V_f in nm³:

$$V_f = 4\pi\Delta R^3/3 \quad (2)$$

For each sample, PAL spectra were obtained at 25°C, each comprising over 1.3×10^6 counts. The spectra were subsequently analyzed with the PALSfit3 program [20], which identified three distinct lifetime components and their corresponding intensities. The most accurate fit for the PAL spectra of the samples was achieved using that program, resulting in three lifetime components and a variance ratio of less than 1.2.

In the model described by Shpotyuk et al. [21], positrons and positronium (Ps) are trapped in two types of defects within the polymer matrix. These trapping rates are denoted by k_{d1} and k_{d2} , as outlined in Equations (3) and (4), whereas k_{d1} corresponds to positron annihilation in defects within the crystalline regions, and k_{d2} corresponds to Ps annihilation in free-volume holes. This differentiation provides insight into the annihilation mechanisms in the various structural regions of the polymer.

$$k_{d1} = I_2 \left(\frac{1}{\tau_1} - \frac{1}{\tau_2} \right) \quad (3)$$

$$k_{d2} = I_3 \left(\frac{1}{\tau_2} - \frac{1}{\tau_3} \right) \quad (4)$$

The combination of precise PAL spectra analysis using PALSfit3 and the theoretical framework provided by Shpotyuk *et al.* offers a highly effective method for characterizing and optimizing the microstructural properties of polymers. This integrated approach enhances our understanding of defect-related phenomena in polymers, paving the way for the development of materials with superior performance characteristics.

Dielectric properties

The dielectric characteristics and AC conductivity of each manufactured membrane were tested as a function of frequency in the 50 Hz–5 MHz range. The instrument used for these tests was the HIOKI-3532 LCR Hi-Tester.

Results and Discussion

FT-IR analysis

Fig. 2a displays the Fourier transform infrared absorption spectra of the PVC/PMMA/SSA sulfonated sample and the PVC/PMMA/SSA sample incorporated with V_2O_5 . First, by comparing the FT-IR spectra of the present blend sample with that of pure PVC and pure PMMA in the literature, one can conclude that an interaction occurred between PVC and PMMA. This is due to the presence of specific absorption bands that were exclusively observed in the spectra of the blend while these bands are not observed for pure PVC and pure PMMA in the literature [22-25]. The observed peaks are detailed as follows; the peak 2940 cm^{-1} shows the vibrational band of $-\text{CH}$ group in PVC. A $-\text{CH}$ wagging mode is observed at the peak 962 cm^{-1} [22, 25]. The observed band at 837 cm^{-1} is related to $\text{C}-\text{Cl}$ stretching mode [22, 23]. The band at 1724 cm^{-1} corresponds to the $\text{C}=\text{O}$ vibrational mode of PMMA [22]. A CH_3 stretching mode appears at the peak 1490 cm^{-1} . In addition to these parent peaks mentioned above, some other peaks were observed in the spectra, the circled peaks, these peaks are related to the sulfonation group SO_3H . The vibrational peaks which appear at the peaks 1040, 1080, and 1180 cm^{-1} arise from $\text{O}-\text{S}-\text{O}$ stretching, and the peak 1320 cm^{-1} arise from SO_3H stretching bands [26].

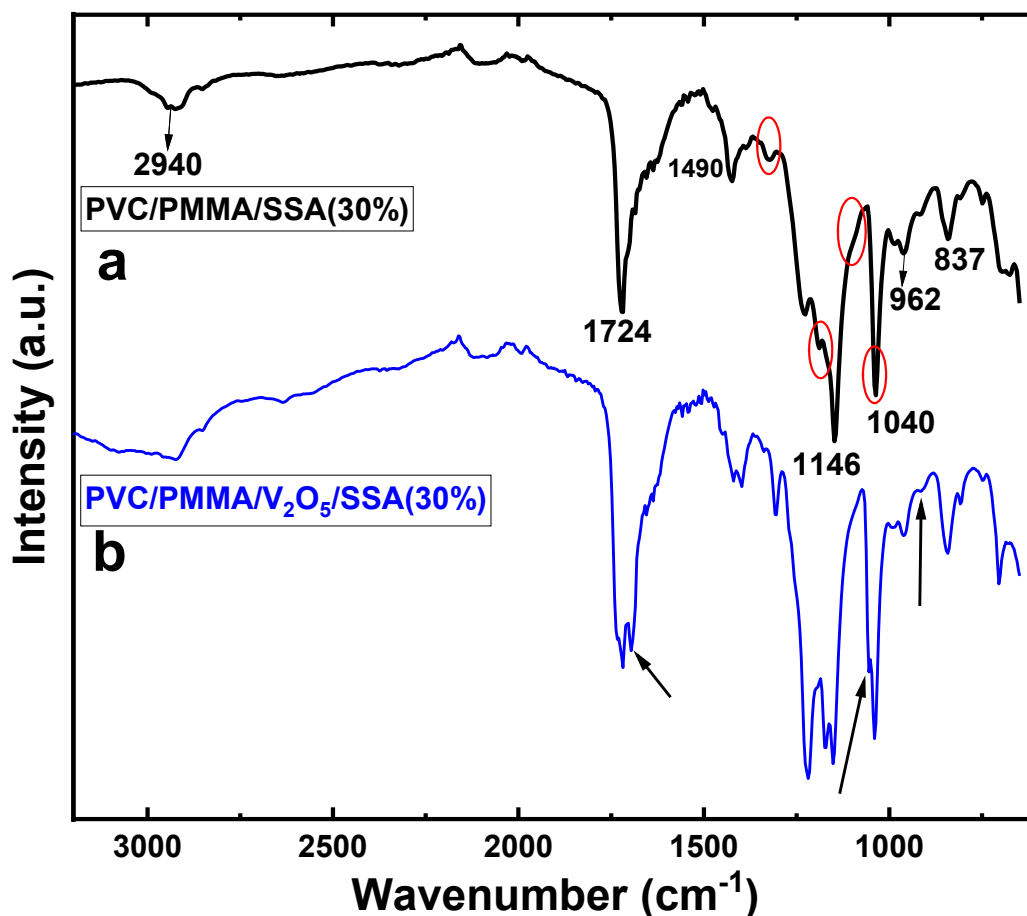


Fig. 2: The FT-IR absorption spectra of sulfonated PVC/PMMA/SSA blend sample and PVC/PMMA/V₂O₅/SSA.

Fig. 2b shows the FT-IR spectra of sulfonated PVC/PMMA blend sample filled with V₂O₅. Listed in the literature that V₂O₅ has a stretching mode (V=O) at the spectrum 1018 cm⁻¹, a stretching mode V-O-V at the peak 829 cm⁻¹, and an asymmetric stretching vibration of triply coordinated oxygen bond is observed at 611 cm⁻¹ [27-30]. In the presence of study, the original peaks 1018 and 829 cm⁻¹ have been shifted to 1055 and 900 cm⁻¹ while the original peak 611 cm⁻¹ has disappeared in the present sample, this clearly indicates the strong chemical reaction between V₂O₅ and the blend PVC/PMMA.

X-ray diffraction investigation

Fig. 3 shows the X-ray diffraction pattern for PVC/PMMA/SSA and PVC/PMMA/V₂O₅/SSA. For both curves, two peaks are observed at positions 12.227° and 25.059°. The position of the two peaks has not changed after adding V₂O₅. This suggests that the PVC/PMMA component is the major factor in determining the peak positions in the XRD pattern. The existence of V₂O₅ has an observable effect on the intensity and broadness of the peaks, which have a lower value compared to the intensity of the PVC/PMMA. This indicates that incorporating V₂O₅ filler into PVC/PMMA led to a slight decrease in the degree of crystallinity of the structure.

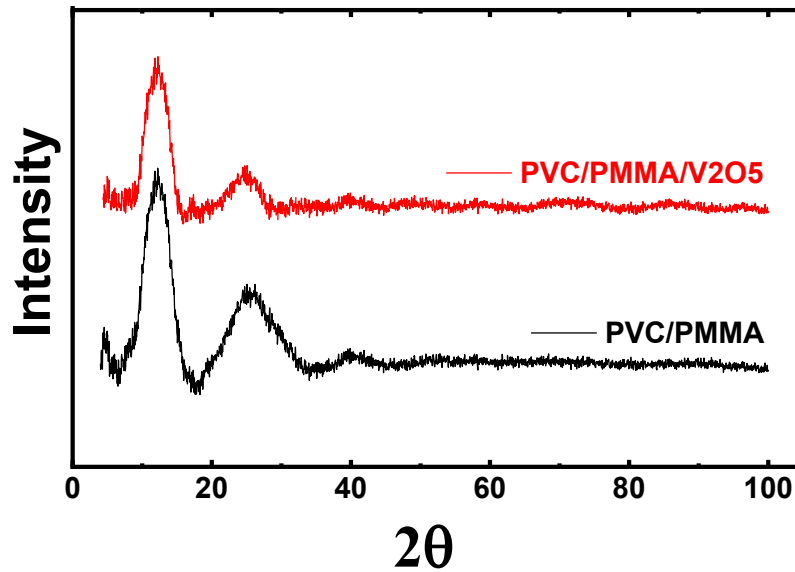


Fig. 3: XRD of PVC/PMMA/SSA (35%) and PVC/PMMA/V₂O₅/SSA (35%)

AC conductivity and conduction mechanism

The AC conductivity appears in a polymer as a result of the movement of the charge carriers inside the chain of the polymer [31]. Fig. 4 exhibits the relationship between the frequency and the ac conductivity of PVC/PMMA/SSA (30%) and PVC/PMMA/V₂O₅/SSA (30%). As observed from the figure, the addition of V₂O₅ to the PVC/PMMA/SSA blend sample led to a decrease in AC conductivity. This is due to the dielectric properties of V₂O₅ where the presence of the dielectric V₂O₅ particles can increase the overall dielectric constant of the structure, which reduces the AC conductivity through the relationship between conductivity and dielectric properties [32]. The Fig. shows two regions with different slopes. The first region, which is attributed to the low frequency, seems to be independent of frequency; this may be attributed to the charge carrier's displacement. The second region demonstrates dispersion resulting from AC conductivity. Jonscher's universal power law defines the relationship between AC conductivity and frequency as follows: [33, 34]:

$$\sigma_{AC}(\omega) = A\omega^s \quad (1)$$

Where σ_{AC} is the AC conductivity, ω is the frequency, A is a temperature-dependent constant that clarifies the polarizability strength, s is an important parameter that helps to identify the conduction mechanism inside the samples, and has values between 0 and 1. For the current samples, the values of s -parameter were calculated from the slope of the straight line in region II and listed in Table 1. The obtained values of s -parameter are less than unity, which indicates that the conduction mechanism is the correlated barrier hopping mechanism (CBH). Numerous investigations in the literature have noted this process [10, 35, 36].

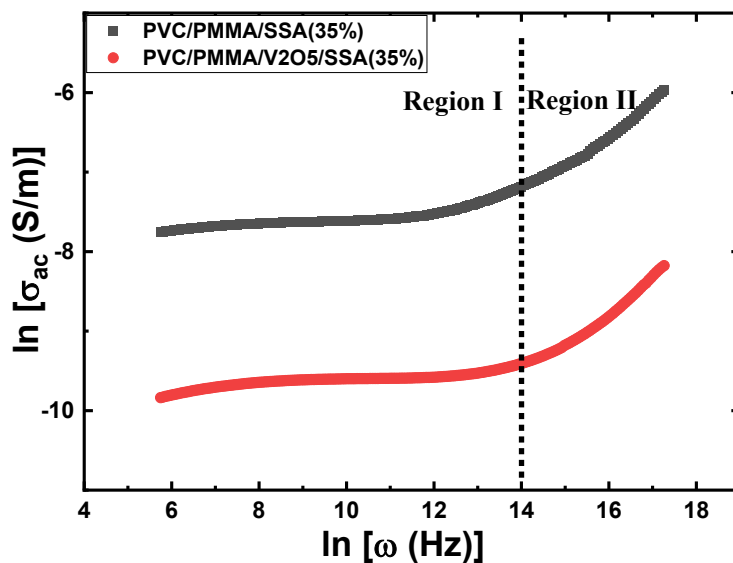


Fig. 4: Frequency dependence of ac conductivity of PVC/PMMA/SSA (35%) and PVC/PMMA/V₂O₅/SSA (35%)

According to the values of the s -parameter, CBH is the major conduction mechanism inside the samples. In this mechanism, the charges need energy to travel through the material, this energy is called barrier height (W_H). In the case of the correlated barrier hopping conduction mechanism, the barrier height (W_H) can be given by the following relation:

$$W_H = \frac{6K_B T}{1-s} \quad (2)$$

In equation 2, K_B is the Boltzmann constant, and T is the temperature. The values of W_H are listed in Table 1. It is observed that W_H of PVC/PMMA/V₂O₅/SSA is higher than that of PVC/PMMA/SSA. As mentioned above, the existence of V₂O₅ can modify the dielectric properties of the structure due to the dielectric property of V₂O₅ which decreases the conductivity of the material and, as a result, increases the barrier height.

Table 1. Measured values of s -parameter and barrier height of the investigated samples

Samples	s -parameter	Barrier height (W_H) (eV)
PVC/PMMA/SSA (30%)	0.365	0.24
PVC/PMMA/V ₂ O ₅ /SSA (30%)	0.382	0.25

Impedance spectroscopy

Fig. 5 exhibits the Cole-Cole plot of the investigated samples. The Fig. shows a semicircle followed by a small straight part, then a small spike at the end of the figure. The semicircle represents the Deby relaxation, and it is electrically represented by an ohmic resistance connected in series with a constant phase element. Such a behavior was observed in a previous study for Ni–Pt–CrO/CNFs [37] and Cr³⁺ substituted ZnAl₂O₄ ceramic [38]. The straight part following the semicircle is typically associated with a constant phase element (CPE). CPE represents a non-ideal capacitance, often due to the distribution of relaxation times or the presence of

heterogeneities in the material. The small spike at the end of the plot represents an inductive element (L). This inductive behavior is usually related to the wiring connections in the measurement setup [39].

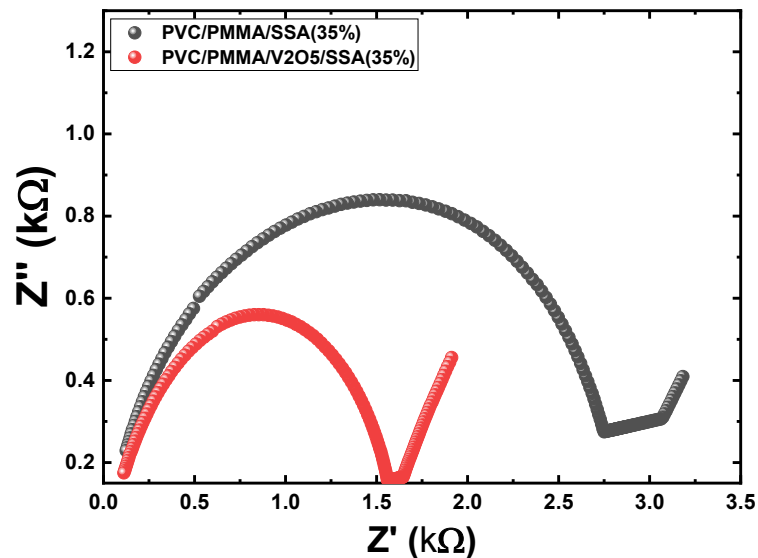


Fig. 5. Cole-Cole plot of PVC/PMMA/SSA (35%) and PVC/PMMA/V₂O₅/SSA (35%)

The dc ionic conductivity of the investigated samples can be calculated as follows:

$$\sigma_{dc} = \frac{d}{R_s a} \quad (3)$$

Where d is the thickness of the sample, a is the effective area of the sample, and R_s represents the charge transfer resistance inside the sample. R_s can be obtained from the intercept of the semicircle with the X-axis. The values of σ_{dc} were calculated for the samples under investigation and found to be $5.24 \times 10^{-4} S/m$ and $7.47 \times 10^{-5} S/m$ for PVC/PMMA/SSA) and PVC/PMMA/V₂O₅/SSA, respectively. It is observed that σ_{dc} is lower for the sample containing V₂O₅. The incorporation of V₂O₅ particles into the PVC/PMMA matrix can lead to strong interactions between the V₂O₅ and the polymer chains. These interactions can restrict the mobility and segmental motion of the polymer chains, which are essential for the transport of ionic charge carriers. As a result, the addition of V₂O₅ impedes the ionic conduction pathways within the polymer blend, leading to a decrease in the overall DC ionic conductivity [17].

PAL Study

Local free volumes in polymeric materials are voids of atomic or molecular dimensions that arise due to the disordered arrangement of the amorphous phase. These voids encompass static and pre-existing cavities resulting from the irregular arrangement of polymer chains. Additionally, the addition of certain materials can induce the formation of dynamic and transient holes through the relaxation of polymer chains and terminal ends. These free volumes play a crucial role in determining the polymer's properties and relaxation behavior, thereby impacting its overall performance and stability. Positron annihilation spectroscopy (PAS) has become a vital technique for investigating structural changes and phase transitions in polymer systems. It is particularly effective in probing free volume hole size V , which relates to the microscopic free volume holes within the polymer matrix. By

analyzing the annihilation characteristics of positrons in these materials, the ortho-positronium lifetime (τ_3) and free volume hole size (V_h) and the trapping rate (K_d) are calculated from equations (1,2&4) and listed in Table 2. In the sulfonated PVC/PMMA sample, the higher τ_3 of 3.15 ns and larger V_h of 216.99 Å³ suggest a more considerable free volume, allowing for more substantial ortho-positronium formation and annihilation times. In contrast, the sulfonated PVC/PMMA/V₂O₅ sample has a τ_3 of 2.55 ns and V_h of 151.85 Å³, reflecting a denser structure with less free volume. The presence of V₂O₅ leads to increased cross-linking and quenching sites, further reducing the τ_3 , and V_h values. The addition of V₂O₅ to the sulfonated PVC/PMMA blend introduces inorganic particles into the polymer matrix. These particles disrupt the packing density of the polymer chains and create physical barriers that prevent the close packing of PMMA and PVC chains [40]. Additionally, the presence of V₂O₅ likely causes microphase separation, where regions of polymer and inorganic particles are distinct. This microphase separation contributes to a decrease in free volume as the polymers cannot pack efficiently around the V₂O₅ particles. The sulfonation process, while introducing sulfonic acid groups that could potentially create some cross-linking and reduce free volume, is outweighed by the disruptive effect of the V₂O₅ particles [18, 41].

Table 2. Ortho-positronium Lifetime τ_3 , free volume hole size (V_h), and Trapping rate (K_d) of the investigated samples

Sample	τ_3 ns	V_h Å ³	(K_d)
Sulfonated PVC/PMMA (SSA 30%)	3.15	216.99	0.27
PVC/PMMA/V ₂ O ₅ (SSA 30%)	2.55	151.85	0.26

The volume fraction hole size distribution for PVC/PMMA/SSA and PVC/PMMA/SSA/V₂O₅ is displayed in Fig. (6). The volume fraction distribution in the PVC/PMMA/SSA sample peaks at approximately 150 Å³, suggesting a greater concentration of free volume holes. This shows that SSA introduces sulfonic acid groups (–SO₃H) by sulfonation, which causes voids and disrupts the polymer chains' ordered structure, resulting in substantial free volume holes. On the other hand, a peak is observed at about 120 Å³ in the PVC/PMMA/SSA/V₂O₅ sample, which suggests a decrease in the size of the free volume hole. This suggests that the addition of V₂O₅ inhibits the creation of bigger free volume holes and encourages microscopic phase separation. The change from 150 Å³ to 120 Å³ indicates that V₂O₅ significantly modifies the dynamics of positron trapping and free volume properties, leading to a more compact and possibly stronger polymer structure.

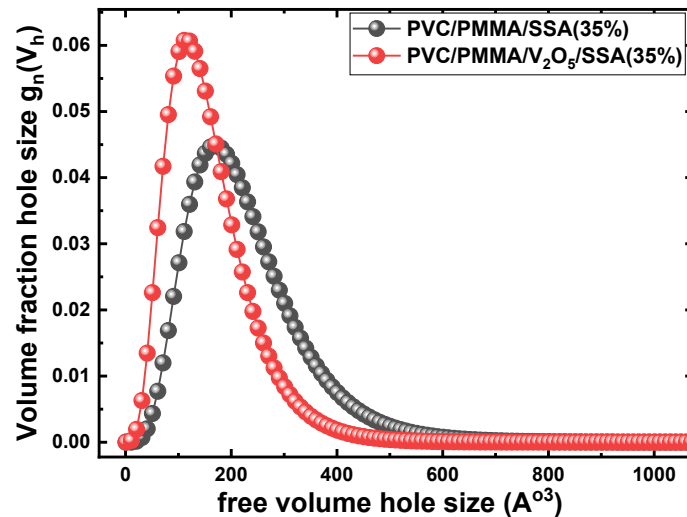


Fig. 6. Normalized free volume distribution $g_n(v_h)$ of sulfonated PVC/PMMA membranes with the free volume hole size V_h

Ionic conductivity depends on the concentration and mobility of charge carriers. In sulfonated PVC/PMMA, the sulfonic acid groups (SO_3H) introduced by SSA play a crucial role in proton conduction. These groups provide sites for proton hopping, creating a continuous network of proton-conducting pathways. The higher proton conductivity in PVC/PMMA/SSA, despite their lower free volume compared to non-sulfonated samples, can be attributed to the efficient proton transport facilitated by the sulfonic acid groups [42, 43]. In the PVC/PMMA/ V_2O_5 sample, the presence of V_2O_5 particles disrupts the continuity of proton-conducting pathways, resulting in lower proton conductivity. The particles create regions of microphase separation and interfere with the formation of a continuous network of sulfonic acid groups. This disruption hinders the formation of efficient proton-conducting pathways, leading to reduced proton conductivity compared to PVC/PMMA/SSA [44]. The incorporation of V_2O_5 into the sulfonated PVC/PMMA matrix significantly influences the free volume, proton conductivity, and crystallinity of the membrane. Sulfonated PVC/PMMA demonstrates higher free volume, proton conductivity, and crystallinity, making it potentially more suitable for applications requiring efficient proton transport. In contrast, sulfonated PVC/PMMA/ V_2O_5 , with its denser structure and reduced crystallinity, may be preferable in scenarios where lower free volume and conductivity are advantageous. Further studies on the morphological and mechanical properties of these membranes would provide a more comprehensive understanding of their performance in various applications [10, 45, 46].

Conclusion

The present study systematically investigates the structural, electrical, and free volume properties of PVC/PMMA blends modified with V_2O_5 filler using a range of characterization techniques, including X-ray diffraction, AC conductivity analysis, impedance spectroscopy, and positron annihilation lifetime spectroscopy. The XRD results reveal that the addition of V_2O_5 to the PVC/PMMA blend does not significantly alter the peak positions, but it decreases the intensity and broadens the peaks, suggesting a slight reduction in the degree of crystallinity. This is attributed to the incorporation of the dielectric V_2O_5 filler within the polymer matrix. The AC conductivity analysis demonstrates that the addition of V_2O_5 leads to a decrease in the AC conductivity of

the PVC/PMMA blend. This is explained by the dielectric properties of V₂O₅, which increase the overall dielectric constant of the structure and reduce the AC conductivity through the relationship between conductivity and dielectric properties. The conduction mechanism is identified as the correlated barrier hopping (CBH) mechanism, where the charge carriers require energy to travel through the material, and the barrier height (WH) is calculated. Impedance spectroscopy analysis reveals a complex impedance response, with a semicircle representing Debye relaxation, a small straight part associated with a constant phase element, and a small spike indicative of an inductive element. The DC ionic conductivity of the PVC/PMMA/V₂O₅ blend is found to be lower than the PVC/PMMA blend, which is attributed to the strong interactions between the V₂O₅ particles and the polymer chains, restricting the mobility and segmental motion of the polymer chains, essential for ionic charge carrier transport. The PALS results show that the addition of V₂O₅ leads to a decrease in the average free volume size and an increase in the free volume fraction compared to the PVC/PMMA blend. This is explained by the reinforcement effect of the V₂O₅ filler, which restricts the segmental motion of the polymer chains and alters the free volume characteristics. The findings from this comprehensive study provide valuable insights into the structure-property relationships in PVC/PMMA blends modified with V₂O₅ filler, with implications for the design and development of advanced polymer-based materials with tailored electrical and free volume properties for various applications, such as energy storage, sensors, and optoelectronics.

References

1. Cao, Jian-Hua, Bao-Ku Zhu, and You-Yi Xu. "Structure and ionic conductivity of porous polymer electrolytes based on PVDF-HFP copolymer membranes." *Journal of Membrane Science*, **281**, 1-2 446-453(2006).
2. David, L., G. Vigier, S. Etienne, A. Faivre, C. L. Soles, and A. F. Yee. "Density fluctuations in amorphous systems: SAXS and PALS results." *Journal of non-crystalline solids*, **235**, 383-387(1998).
3. Hosseini, S. M., B. Rahzani, H. Asiani, A. R. Khodabakhshi, A. R. Hamidi, S. S. Madaeni, A. R. Moghadassi, and A. Seidy-poor. "Surface modification of heterogeneous cation exchange membranes by simultaneous using polymerization of (acrylic acid-co-methyl methacrylate): Membrane characterization in desalination process." *Desalination*, **345**, 13-20(2014).
4. Stephan, A. Manuel. "Review on gel polymer electrolytes for lithium batteries." *European polymer journal*, **42** (1), 21-42 (2006).
5. Zhang, Haoqin, Chuanming Ma, Jingtao Wang, Xuyang Wang, Huijuan Bai, and Jindun Liu. "Enhancement of proton conductivity of polymer electrolyte membrane enabled by sulfonated nanotubes." *International journal of hydrogen energy*, **39**(2), 974-986 (2014).
6. Lu, Yanying, Yeting Wen, Fei Huang, Tianyu Zhu, Shichen Sun, Brian C. Benicewicz, and Kevin Huang. "Rational design and demonstration of a high-performance flexible Zn/V2O5 battery with thin-film electrodes and para-polybenzimidazole electrolyte membrane." *Energy Storage Materials*, **27**, 418-425(2020).
7. Dixit, Manasvi, Vishal Mathur, Sandhya Gupta, Mahesh Baboo, Kananbala Sharma, and N. S. Saxena. "Investigation of miscibility and mechanical properties of PMMA/PVC blends." *J. Optoelectron. Adv. Mater. Rapid Commun*, **3** (10), 1099-1105(2009).
8. Awad, Somia, Esam E. Abdel-Hady, Hamdy FM Mohamed, Yehya S. Elsharkawy, and Mahmoud M. Goma. "Non-fluorinated PVA/SSA proton exchange membrane studied by positron annihilation technique for fuel cell application." *Polymers for advanced Technologies*, **32** (8), 3322-3332(2021).
9. Jean, Y. C., J. David Van Horn, Wei-Song Hung, and Kuier-Rarn Lee. "Perspective of positron annihilation spectroscopy in polymers." *Macromolecules* **46** (18), 7133-7145(2013).

10. Mohammed, Wael M., Somia Awad, Esam E. Abdel-Hady, Hamdy FM Mohamed, Yehya S. Elsharkawy, and Mohamed RM Elsharkawy. "Nanostructure analysis and dielectric properties of PVA/sPTA proton exchange membrane for fuel cell applications: Positron lifetime study." *Radiation Physics and Chemistry*, **208**, 110942 (2023).
11. Wada, Ken, and Toshio Hyodo. "A simple shape-free model for pore-size estimation with positron annihilation lifetime spectroscopy." In *Journal of Physics: Conference Series*, vol. 443, no. 1, p. 012003. IOP Publishing, 2013.
12. Bigg, D. M. "A review of positron annihilation lifetime spectroscopy as applied to the physical aging of polymers." *Polymer Engineering & Science* 36, no. 6 (1996): 737-743.
13. Eldrup, Morten, D. Lightbody, and John Neil Sherwood. "The temperature dependence of positron lifetimes in solid pivalic acid." *Chemical Physics* 63, no. 1-2 (1981): 51-58.
14. Alsaiani, Mabkhoot A., Mohamed Morsy, Mona Samir, Abdulaziz Al-Qahtani, Rami Aslsaiani, Ali Alsaiani, Elbadawy A. Kamoun, Ahmed I. Ali, and Galal H. Ramzy. "Advantages incorporating V2O5 nanoparticles into PMMA composite membranes for the structural, optical, electrical, and mechanical properties for conductive polymeric membrane applications." *Mater. Adv* 5 (2024): 3297-3308.
15. Hu, Peng, Ping Hu, Tuan Duc Vu, Ming Li, Shancheng Wang, Yujie Ke, Xianting Zeng, Liqiang Mai, and Yi Long. "Vanadium oxide: phase diagrams, structures, synthesis, and applications." *Chemical Reviews* 123, no. 8 (2023): 4353-4415.
16. André, Rute, Filipe Natálio, Madalena Humanes, Jana Leppin, Katja Heinze, Ron Wever, H-C. Schröder, Werner EG Müller, and Wolfgang Tremel. "V2O5 nanowires with an intrinsic peroxidase-like activity." *Advanced Functional Materials* 21, no. 3 (2011): 501-509.
17. Elsharkawy, M., et al., Characterization of vacancy defects in Cu (In, Ga) Se₂ by positron annihilation spectroscopy. *AIP Advances*, 2016. 6(12).
18. Gomaa, M. M., Hugenschmidt, C., Dickmann, M., Abdel-Hady, E. E., Mohamed, H. F., & Abdel-Hamed, M. O. (2018). Crosslinked PVA/SSA proton exchange membranes: Correlation between physiochemical properties and free volume determined by positron annihilation spectroscopy. *Physical Chemistry Chemical Physics*, 20(44), 28287-28299.
19. Mohamed, H. F., Abdel-Hady, E. E., & Mohammed, W. M. (2022). Investigation of Transport Mechanism and Nanostructure of Nylon-6, 6/PVA Blend Polymers. *Polymers*, 15(1), 107.
20. Olsen, J. V., Peter Kirkegaard, and M. Eldrup. "Analysis of positron lifetime spectra using the PALSfit3 program." In *AIP Conference Proceedings*, vol. 2182, no. 1. AIP Publishing, 2019.
21. Hammannavar, Preeti B., Blaise Lobo, and P. M. G. Nambissan. "Positron annihilation studies of free volume changes accompanying the incorporation of lead nitrate in PVA-PVP polymeric blend." *Radiation Physics and Chemistry* 158 (2019): 53-60.
22. Rajendran, S., & Uma, T. (2000). Conductivity studies on PVC/PMMA polymer blend electrolyte. *Materials Letters*, 44(3-4), 242-247.
23. Ramesh, S., & Liew, C. W. (2013). Development and investigation on PMMA–PVC blend-based solid polymer electrolytes with LiTFSI as dopant salt. *Polymer bulletin*, 70, 1277-1288.
24. Ramesh, S., Leen, K. H., Kumutha, K., & Arof, A. K. (2007). FTIR studies of PVC/PMMA blend based polymer electrolytes. *Spectrochimica Acta Part A: Molecular and Biomolecular Spectroscopy*, 66(4-5), 1237-1242.
25. Khutia, M., & Joshi, G. M. (2015). Dielectric relaxation of PVC/PMMA/NiO blends as a function of DC bias. *Journal of Materials Science: Materials in Electronics*, 26, 5475-5488.
26. Jadhav, A. H., Lee, K., Koo, S., & Seo, J. G. (2015). Esterification of carboxylic acids with alkyl halides using imidazolium based dicationic ionic liquids containing bis-trifluoromethane sulfonimide anions at room temperature. *RSC Advances*, 5(33), 26197-26208.
27. Kang, W., Yan, C., Wang, X., Foo, C. Y., Tan, A. W. M., Chee, K. J. Z., & Lee, P. S. (2014). Green synthesis of nanobelt-membrane hybrid structured vanadium oxide with high electrochromic contrast. *Journal of Materials Chemistry C*, 2(24), 4727-4732.
28. Jadhav, C. D., Pandit, B., Karade, S. S., Sankapal, B. R., & Chavan, P. G. (2018). Enhanced field emission properties of V₂O₅/MWCNTs nanocomposite. *Applied Physics A*, 124, 1-8.

29. Xavier, J. R. (2021). High protection performance of vanadium pentoxide-embedded polyfuran/epoxy coatings on mild steel. *Polymer Bulletin*, **78**(10), 5713-5739.
30. Surya Bhaskaram, D., Cheruku, R. and Govindaraj, G. (2016). Reduced graphene oxide wrapped V₂O₅ nanoparticles: green synthesis and electrical properties. *Journal of Materials Science: Materials in Electronics*, **27**, 10855-10863.
31. Dyre, J. C. and Schröder, T. B. (2000). Universality of ac conduction in disordered solids. *Reviews of Modern Physics*, **72**(3), 873.
32. Ray, A., Roy, A., De, S., Chatterjee, S. and Das, S. (2018). Frequency and temperature dependent dielectric properties of TiO₂-V₂O₅ nanocomposites. *Journal of Applied Physics*, **123**(10).
33. Hmamm, M. F. M., Zedan, I. T., Mohamed, H. F., Hanafy, T. A. and Bekheet, A. E. (2021) Study of the nanostructure of free volume and ionic conductivity of polyvinyl alcohol doped with NaI. *Polymers for Advanced Technologies*, **32**(1), 173-182.
34. Karmakar, S. and Behera, D. (2020) Band-correlated barrier-hopping conduction in α -NiMoO₄ micro-crystals and comparison of its energy storage performance with MWCNT-integrated complex. *Journal of Materials Science: Materials in Electronics*, **31**(7), 5336-5352.
35. Li, K., Xia, Y., Xu, B., Gao, X., Guo, H., Liu, Z. and Yin, J. (2010) Conduction behavior change in amorphous LaLuO₃ dielectrics based on correlated barrier hopping theory. *Applied Physics Letters*, **96**(18).
36. Abdel-Hady, E. E., Gamal, A., Hamdy, H., Shaban, M., Abdel-Hamed, M. O., Mohammed, M. A., & Mohammed, W. M. (2023) Methanol electro oxidation on Ni-Pt-CrO/CNFs composite: morphology, structural, and electrochemical characterization. *Scientific Reports*, **13**(1), 4870.
37. Elhamdi, I., Mselmi, F., Souissi, H., Kammoun, S., Dhahri, E., Sanguino, P., & Costa, B. F. O. (2023). Summerfield scaling model and electrical conductivity study for understanding transport mechanisms of a Cr³⁺ substituted ZnAl₂O₄ ceramic. *RSC advances*, **13**(5), 3377-3393.
38. Cha, J. R., & Gong, M. S. (2013). AC complex impedance study on the resistive humidity sensors with ammonium salt-containing polyelectrolyte using a different electrode pattern. *Bulletin of the Korean Chemical Society*, **34**(9), 2781-2786.
39. Rajendran, S., Kannan, R. and Mahendran, O. (2001) Ionic conductivity studies in poly (methylmethacrylate)-polyethylene oxide hybrid polymer electrolytes with lithium salts. *Journal of power sources*, **96**(2), 406-410.
40. Schmidt, M., and F. H. J. Maurer. "Relation between free-volume quantities from PVT-EOS analysis and PALS." *Polymer*, **41**(23), 8419-8424(2000).
41. Kobayashi, Y., A. Kinomura, S. Kazama, K. Inoue, T. Toyama, Y. Nagai, K. Haraya et al. "Hole size distributions in cardo-based polymer membranes deduced from the lifetimes of ortho-positronium." In *Journal of Physics: Conference Series*, **674** (1), p. 012017. IOP Publishing, 2016.
42. James, Jose, George V. Thomas, Akhil Punneri Madathil, P. M. G. Nambissan, Nandakumar Kalarikkal, and Sabu Thomas. "Positron annihilation spectroscopic characterization of free-volume defects and their correlations with the mechanical and transport properties of SBR-PMMA interpenetrating polymer networks." *Physical Chemistry Chemical Physics*, **22**, (32) 18169-18182(2020).
43. El-Gamal, S., and M. Elsayed. "Synthesis, structural, thermal, mechanical, and nano-scale free volume properties of novel PbO/PVC/PMMA nanocomposites." *Polymer*, **206**, 122911(2020).
44. Sutton, L., J. Lauzier, and J. De la Venta. "Magnetic properties of hybrid V₂O₃/Ni composites." *Journal of Applied Physics*, **123**(8) (2018).
45. Liu, J., Y. C. Jean, and H. Yang. "A Positron-Annihilation-Lifetime Study of Polymer Blends." *MRS Online Proceedings Library (OPL)* **321**, 47(1993).
46. Kruse, J., J. Kanzow, K. Rätzke, F. Faupel, M. Heuchel, J. Frahn, and D. Hofmann. "Free volume in polyimides: positron annihilation experiments and molecular modeling." *Macromolecules*, **38** (23) 9638-9643(2005).